Journal of
Materials Chemistry A

Materials for energy and sustainability

Accepted Manuscript

This article can be cited before page numbers have been issued, to do this please use: G. Sun, W. Qian, J. Jiao, T. Han, Y. Shi, X. Hu and L. Wang, *J. Mater. Chem. A*, 2020, DOI: 10.1039/D0TA03169K.

ROYAL SOCIETY OF CHEMISTRY

rsc.li/materials-a

View Article Online
DOI: 10.1039/D0TA03169K

ARTICLE

Highly efficient artificial light-harvesting system with two-step sequential energy transfer based on supramolecular self-assembly

Guangping Sun,[a] Weirui Qian,[a] Jianmin Jiao,[a] Tingting Han,[c] Yukun Shi,[a] Xiao-Yu Hu*[b] and Leyong Wang*[a,d]

A highly efficient artificial light-harvesting system (ALHS) in aqueous phase with two-step sequential energy transfer process has been successfully constructed based on the host–guest interaction between a water-soluble pillar[5]arene (**WP5**) and a bola-type bis(4-phenyl)acrylonitrile derivative (**BPT**), as well as two different hydrophobic fluorescnet dyes (4,7-bis(thien-2-yl)-2,1,3-benzothiadiazole (**DBT**) and Nile Red (**NiR**)). The fabricated ALHS shows an ultrahigh antenna effect (47.8 for the first step and 20.1 for the second step) with a high donor/acceptor ratio of 350:1. It is noted that the obtained **WP5⊃BPT** supramolecular nanoparticles possess enhanced aggregation-induced emission (AIE) effect and can function as an ideal donor to realize the first-step of energy transfer from the **WP5⊃BPT** assembly to **DBT**. Moreover, inspired by the sequential energy transfer in nature, **NiR** was carefully selected as the second acceptor to fabricate an efficient two-step sequential light-harvesting system based on **WP5⊃BPT-DBT-NiR** assembly, which exhibits a high FRET efficiency of 60.9% and 89.4% for the two-step sequential energy transfer process, respectively. Notably, the emission color changed from light blue to bright green and then to bright red during this process, thus by tuning the molar ratio of **DBT** and **NiR**, a bright white light emission can be achieved with a high fluorescence quantum yield of 23.5%, which showed a strong ability of white fluorescence emission and promising applications in visible-light photocatalysis.

Received 00th January 20xx,
Accepted 00th January 20xx

DOI: 10.1039/x0xx00000x

Introduction

In recent years, solar energy, as a kind of inexhaustible clean energy, has attracted more and more attention from science and technology.[1,2] Inspired by green plants and some photosynthetic bacteria in nature,[3–6] which can capture, transfer, and store solar energy effectively to achieve photosynthesis, a series of artificial light-harvesting systems (ALHSs) have been developed, such as dendrimers,[7–9] organic gels,[10–12] porphyrin arrays/assemblies,[13–16] biomaterials,[17–20] and organic-inorganic hybrid materials.[21–24] However, most of these ALHSs have performed in organic solvents due to the intrinsic hydrophobic effect and their conventional chromophores (donor), which always suffer from aggregation-caused quenching (ACQ) effect in aqueous solution, thus greatly limiting their application in mimicking natural systems.[25] In natural photosynthesis, more than 200 antenna chromophores (donor) can absorb light energy and transfer it to one acceptor at the reaction center,[26–30] such a high donor/acceptor ratio is still a challenge for conventional ACQ chromophore in fabricating ALHSs in aqueous solution. Fortunately, in 2001, Tang and co-workers observed the phenomenon of aggregation-induced emission (AIE) effect that is exactly opposite to the ACQ effect.[31] In the AIE process, the chromophores are almost nonfluorescent in the molecular state, but become highly emissive in the aggregate state.[32-37] Moreover, it is noteworthy that the efficient natural light-harvesting systems are constructed by the noncovalent interactions between chlorophyll and protein.[38] Therefore, compared with traditional ALHSs which are constructed via covalent bonds,[39–46] supramolecular light-harvesting systems constructed by noncovalent interaction can not only avoid multiple steps of synthesis and purification during the structure fabrication, but also can be successfully achieved in aqueous solution, showing more potential in artificial light-harvesting.[47–55]

For example, in 2017, Liu and co-workers reported an efficient supramolecular ALHS constructed by an AIE molecule, an oligo(phenylenevinylene) derivative (**OPV-I**), and a supramolecular macrocycle, sulfato-β-cyclodextrin (**SCD**), which performed an extremely high antenna effect of 32.5.[51] Besides, in 2018, our group also fabricated two highly efficient

[a] Key Laboratory of Mesoscopic Chemistry of MOE, Jiangsu Key Laboratory of Advanced Organic Materials, School of Chemistry and Chemical Engineering, Nanjing University, Nanjing 210023, China. E-mail: lywang@nju.edu.cn
[b] College of Material Science and Technology, Applied Chemistry Department, Nanjing University of Aeronautics and Astronautics, Nanjing 211100, China. E-mail: huxy@nuaa.edu.cn
[c] State Key Laboratory of Analytical Chemistry for Life Science, School of Chemistry and Chemical Engineering, Nanjing University, Nanjing 210023, China.
[d] School of Petrochemical Engineering, Changzhou University, Changzhou 213164, China.

Electronic Supplementary Information (ESI) available: [details of any supplementary information available should be included here]. See DOI: 10.1039/x0xx00000x

supramolecular ALHSs based on the self-assembly of a water-soluble pillar[6]arene (**WP6**), a salicylaldehyde azine derivative (**G**), and two types of fluorescence dye (Nile red (**NiR**) or Eosin Y (**ESY**)), which showed a high antenna effect of 25.4 and 28.0, respectively.[52] However, most of these systems only involve one-step direct Förster resonance energy transfer (FRET) process from the donor to acceptor, while the natural light-harvesting system with excellent efficiency is characterized by multi-channel information communication.[56,57] Up to now, only a few examples of two-step sequential light-harvesting systems have been fabricated in aqueous environment based on supramolecular self-assembly.[38,58,59] In 2019, we have designed a two-step sequential energy transfer system based on a water-soluble pillar[5]arene (**WP5**) and a tetraphenylethylene-functionalized dialkyl ammonium derivative (**TPEDA**).[38] But the antenna effect of this two-step sequential light-harvesting system was only 11.5 and 3.5, respectively. Therefore, it is still a very challenging task to design and fabricate highly efficient sequential light-harvesting systems in aqueous environment.

Herein, we report a novel two-step sequential ALHS based on noncovalent supramolecular self-assembly between **WP5** and a bola-type bis(4-phenyl)acrylonitrile derivative (**BPT**), which could efficiently realize two-step sequential energy transfer process in aqueous environment (Fig. 1). As a classical type of AIE molecule, **BPT** in the aggregated form can exhibit high emission and will be an ideal donor for light-harvesting in aqueous phase.[56,60–62] Meanwhile, considering the brilliant property of host–guest chemistry and solubility, **WP5** will be an excellent host for **BPT** to lower its critical aggregation concentration and significantly strengthen its AIE effect in water. As shown in Fig. 1, based on the host–guest interaction, **WP5** could directly bind with **BPT** and further self-assembled into **WP5**⊃**BPT** nanoparticles, which showed blue fluorescence when excited at 365 nm. Simultaneously, 4,7-bis(thien-2-yl)-2,1,3-benzothiadiazole (**DBT**),[48,50] as a hydrophobic energy acceptor, was successfully encapsulated into the hydrophobic core of the formed **WP5**⊃**BPT-DBT** nanoparticles, which was mainly driven by cooperative hydrophobic, C-H···π and π-π stacking interactions. Moreover, since the fluorescence emission band of the **WP5**⊃**BPT** nanoparticles overlaps very well with the absorption band of **DBT**, an efficient one-step energy transfer process took place from the **WP5**⊃**BPT** complex to **DBT**, which was characterized by the observation of strong green fluorescence. Furthermore, **NiR**,[38,51,52] another hydrophobic fluorescent dye, was carefully selected as the second energy acceptor to realize the two-step sequential energy transfer process, which was confirmed by the observation of obvious fluorescence changing from green to red. Therefore, such a two-step sequential energy transfer system (**WP5**⊃**BPT-DBT-NiR** assembly) could initially take place from the **WP5**⊃**BPT** complex to **DBT** and then to **NiR** with a high energy transfer efficiency of 60.9% and 89.4%, respectively. Moreover, this ALHS showed an ultrahigh antenna effect of 47.8 for the first step and 20.1 for the second step with a high donor/acceptor ratio ([**BPT**]/[**DBT**] =

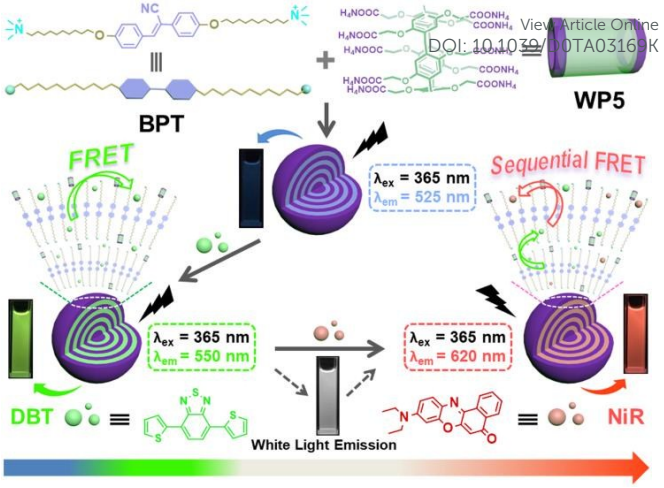

Fig. 1 Schematic illustration of supramolecular self-assembly of artificial light-harvesting system with two-step sequential energy transfer in aqueous solution.

350:1 and [**BPT**]/[**DBT**]/[**NiR**] = 350:1:1). Notably, a strong white light emission could be successfully achieved during this sequential energy transfer process with a high fluorescent quantum yield of 23.5%. More importantly, based on the AIE enhanced FRET efficiency, undesired fluorescence self-quenching could be effectively avoided and two-step as well as multi-step sequential energy transfer process could be realized in aqueous solution, thus the present work showed great potential in mimicking natural photosynthesis based on supramolecular chemistry.

Results and discussion

Investigation of host–guest complexation

As shown in Fig. S1 and S2 (ESI†), **WP5** was synthesized according to the reported literatures,[63–66] and **BPT** was obtained by a two-step reaction using 4-((10-bromodecyl)oxy)benzaldehyde as the starting material.[40,51,56,67] Initially, considering the complicated structure of **BPT** may hamper the investigation of host–guest interaction with **WP5**, $\mathbf{G_M}$, a model guest molecule with the same binding site as **BPT** (Fig. S11, ESI†), was synthesized to investigate the complexation between **BPT** and **WP5**.[64] As shown in Fig. 2, all the resonance signals of $\mathbf{G_M}$ exhibited significantly upfield chemical shifts, while **WP5** showed slightly downfield chemical shifts, indicating that **BPT** could bind well with **WP5** to form a supramolecular inclusion complex. Simultaneously, isothermal titration calorimetry (ITC) was performed to quantitatively assess the exact binding property between **WP5** and $\mathbf{G_M}$ (Fig. 3). Based on the obtained ITC data, the stoichiometry between **WP5** and $\mathbf{G_M}$ was confirmed to be 1:1 and the association constant (K_a) was calculated to be (4.27 ± 1.22) × 10^4 M^{-1}. Considering the similar binding site of **BPT** with **WP5**, we deduced the association constant between **BPT** and **WP5** should be estimated to be about 10^4 M^{-1}, which might be

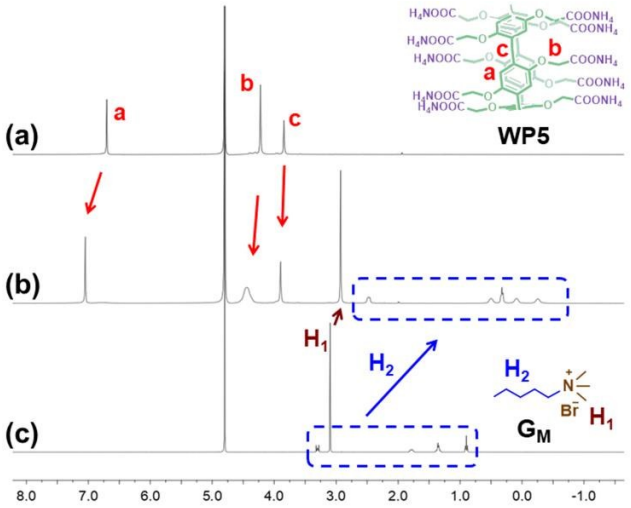

Fig. 2 ^{1}H NMR (400 MHz, D_2O, 298 K) spectra: (a) **WP5** (8.0 mM), (b) **WP5** (8.0 mM), $\mathbf{G_M}$ (4.0 mM), and (c) $\mathbf{G_M}$ (4.0 mM).

mainly driven by the cooperative hydrophobic, electrostatic, and CH-π interactions.[68–71]

Construction of supramolecular nanoparticles based on WP5⊃BPT complex

Before exploring the energy transfer process, dynamic light scattering (DLS) experiment was firstly carried out to investigate the aggregating behavior of **WP5⊃BPT** complex in water. Initially, almost no signal could be observed for free **BPT** aqueous solution (1×10^{-4} M, containing 0.2 % DMSO), indicating no aggregates assembled in free **BPT** solution. Meanwhile, no obvious fluorescence could be detected for the free **BPT** solution, suggesting that free **BPT** was hard to self-assemble into nanoaggregates under the measured condition (Fig. S12, ESI†). However, when **WP5** was added into the free **BPT** solution, a light opalescence and clear Tyndall effect could be observed immediately (Fig. 4a and S13, ESI†), suggesting the existence of abundant nanoaggregates. Moreover, the **WP5⊃BPT** solution showed significantly enhanced blue fluorescence (Fig. S12, ESI†), confirming that **WP5** could induce the self-assembly of **BPT** at low concentration, resulting in the obvious AIE effect in return. And the best molar ratio between **BPT** and **WP5** for aggregation was further determined to be 5:1 by the optical transmittance experiments (Fig. S14, ESI†).[38,51,52] Based on this host–guest molar ratio, the critical aggregation concentration (CAC) of **WP5⊃BPT** solution was determined to be 0.1 mM (Fig. S15, ESI†).

Subsequently, the size and morphology of these supramolecular nanoaggregates were explored by DLS and transmission electron microscopy (TEM) measurements. DLS results revealed that the nanoaggregates formed by **WP5⊃BPT** complex had a narrow size distribution with an average hydrodynamic diameter of 180 nm (Fig. 4a). And TEM images clearly showed the morphology of a dark spherical structure with diameters ranging from 150 to 200 nm, indicating the formation of multilayered spherical core-shell structure as

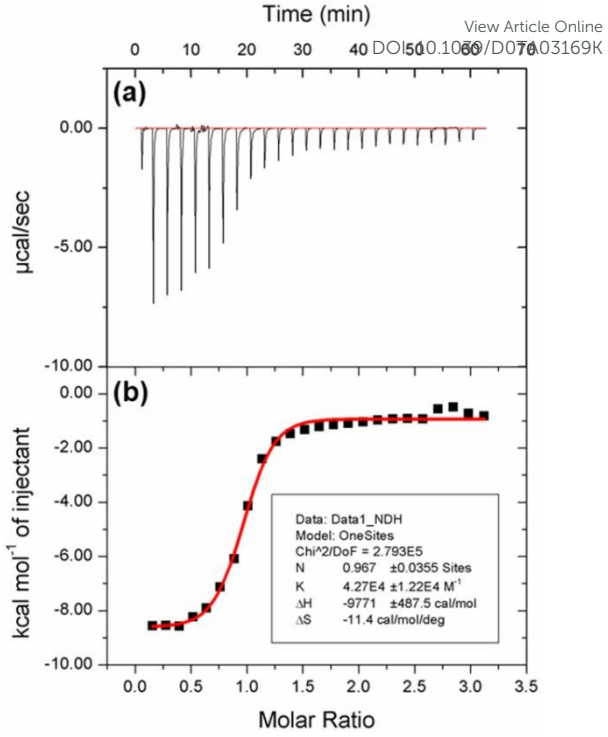

Fig. 3 Microcalorimetric titrations of **WP5** with $\mathbf{G_M}$ in water at 298 K. (a) Raw ITC data of microcalorimetric titrations for 25 sequential injections (1.5 μL per injection) of **WP5** solution (6 mM) into the aqueous solution of $\mathbf{G_M}$ (0.6 mM); (b) "S-type" heat effects of the complexation between **WP5** and $\mathbf{G_M}$ for each injection, obtained by subtracting the dilution heat from the reaction heat, which was fitted by computer simulation using the "one set of binding sites" model.

illustrated in Fig. 1 (Fig. 4d). Subsequently, zeta-potential assays showed that the obtained **WP5⊃BPT** nanoparticle solution possessed a relatively high positive ζ- potential (46.94 mV), suggesting the strong repulsive forces around the surfaces of the **WP5⊃BPT** nanoparticles can prevent their agglomeration in aqueous solution (Fig. S16, ESI†).

Investigation of the one-step energy transfer process of WP5⊃BPT-DBT nanoparticles

Since **WP5** could obviously induce the enhanced AIE effect of **BPT** with fluorescence quantum yield of 3.28% (Fig. S19, ESI†), **WP5⊃BPT** nanoparticles could be used as an ideal donor to construct artificial light-harvesting systems in aqueous phase, which could effectively avoid the conventional fluorescence self-quenching of the aggregated donor chromophores in water. **DBT**, a hydrophobic fluorescence dye, was firstly selected as the fluorescent acceptor due to the good overlap between the absorption band of **DBT** with the emission band of **WP5⊃BPT** nanoparticles (Fig. S17, ESI†). Moreover, **DBT** could be successfully encapsulated into the hydrophobic layer of the **WP5⊃BPT** nanoparticles to form tightly stacked π-π stacking assembly, which significantly shortened the distance between the donor and the acceptor, making it possible for

View Article Online
DOI: 10.1039/D0TA02169K

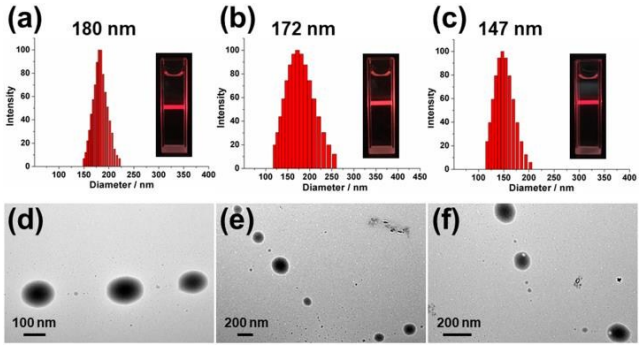

Fig. 4 DLS data: (a) **WP5⊃BPT** nanoparticles, (b) **WP5⊃BPT-DBT** nanoparticles, and (c) **WP5⊃BPT-DBT-NiR** nanoparticles. TEM images: (d) **WP5⊃BPT** nanoparticles, (e) **WP5⊃BPT-DBT** nanoparticles, and (f) **WP5⊃BPT-DBT-NiR** nanoparticles. [**WP5**] = 2×10^{-5} M, [**BPT**] = 1×10^{-4} M, [**DBT**] = 2.8×10^{-7} M, and [**NiR**] = 2.8×10^{-7} M, respectively.

achieving the FRET process with high efficiency. As shown in Fig. 5, with gradual addition of **DBT** to the **WP5⊃BPT** nanoparticles, the fluorescence intensity of the **WP5⊃BPT** nanoparticles (donor) at 450 nm decreased obviously, while the fluorescence emission of **DBT** (acceptor) at 550 nm increased significantly when excited at 365 nm. Moreover, the fluorescence emission changed from light blue to bright green (Fig. 5b and S26, ESI†). The above phenomena indicated the efficient energy transfer had taken place from the **WP5⊃BPT** assembly (donor) to the encapsulated **DBT** (acceptor). Simultaneously, the fluorescence quantum yield of **WP5⊃BPT-DBT** nanoparticles also showed a notable increase (16.85%; Fig. S19, ESI†), probably because **DBT** could accept and emit the maximum possible amount of excitation energy,[52] corresponding to the above process of energy transfer.

In order to further confirm the light harvesting process, fluorescence decay experiments were conducted. The decay curve of the **WP5⊃BPT** nanoparticles was fitted as a double exponential decay, which showed the fluorescence lifetimes of τ_1 = 0.60 ns and τ_2 = 2.80 ns when emitting at 450 nm (Fig. 5b

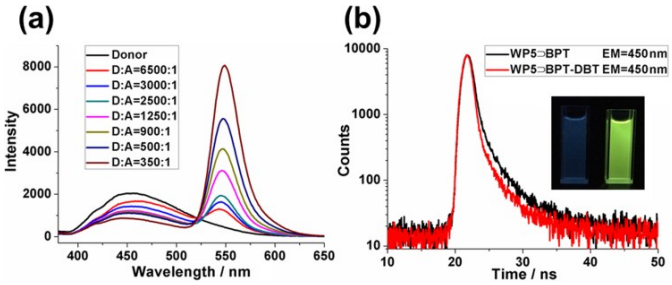

Fig. 5 (a) Fluorescence spectra of **WP5⊃BPT** nanoparticles in water with different concentrations of **DBT**. (b) Fluorescence decay profiles of **WP5⊃BPT** nanoparticles (black line) and **WP5⊃BPT-DBT** nanoparticles (red line). Inset: photographs of **WP5⊃BPT** nanoparticles and **WP5⊃BPT-DBT** nanoparticles. [**WP5**] = 2×10^{-5} M, [**BPT**] = 1×10^{-4} M, and [**DBT**] = 2.8×10^{-7} M, respectively.

and Table S1, ESI†). However, the fluorescence lifetimes of the **WP5⊃BPT-DBT** nanoparticles decreased to τ_1 = 0.40 ns and τ_2 = 2.42 ns when emitting at 450 nm, indicating that the **WP5⊃BPT-DBT** artificial light-harvesting system had been successfully constructed and the energy could be efficiently transferred from the **WP5⊃BPT** assembly (donor) to the acceptor **DBT** (Table S1, ESI†). Subsequently, in order to quantitatively evaluate the ability of this ALHS, it is necessary to investigate the energy transfer efficiency and antenna effect[38,48,50–52]. According to the fluorescence quenching ratio of the **WP5⊃BPT** nanoparticles at 450 nm, the energy transfer efficiency was calculated to be 60.9% with the molar ratio of donor/acceptor = 350:1 (Fig. S20, ESI†). Furthermore, the antenna effect was calculated to be 47.8 at such a high donor/acceptor ratio (Fig. S22, ESI†), indicating the fabricated **WP5⊃BPT-DBT** nanoparticles could function as an excellent light-harvesting antenna in aqueous environment.

Investigation of the two-step energy transfer process of WP5⊃BPT-DBT-NiR nanoparticles

Inspired by the photosynthetic light-harvesting systems in nature, multi-step sequential energy transfer rather than the simple one-step energy transfer become more meaningful for ALHSs.[3,38] Therefore, based on the obtained efficient one-step energy transfer of the **WP5⊃BPT-DBT** nanoparticles, two-step sequential energy transfer process was further investigated. Based on careful literature survey,[38,51,52,72] **NiR**, another hydrophobic fluorescence dye, was found quite suitable for the second-step sequential light-harvesting system due to the fact that the absorption band of **NiR** overlaps very well with the emission band of the **WP5⊃BPT-DBT** nanoparticles. Accordingly, when the second acceptor **NiR** was gradually added into the **WP5⊃BPT-DBT** nanoparticles, the fluorescence intensity of **DBT** at 550 nm decreased remarkably and the fluorescence emission of **NiR** (the second acceptor) at 620 nm increased significantly when excited at 365 nm (Fig. 6a). Meanwhile, the fluorescence emission changed from bright green to bright red (Fig. 6b and S26, ESI†). These results showed that two-step sequential energy transfer process took place from the **WP5⊃BPT-DBT** nanoparticles to the second acceptor **NiR**. Notably, **DBT**, as a key bridge, was first used to realize this sequential energy transfer process in aqueous light-harvesting system (Fig. S27, ESI†). Furthermore, compared to the **WP5⊃BPT-DBT** nanoparticles, the fluorescence quantum yield of the **WP5⊃BPT-DBT-NiR** nanoparticles showed a significant increase again (31.6%) (Fig. S19, ESI†), confirming the occurrence of this two-step energy transfer process. The energy transfer efficiency was then calculated to be 89.4% with the molar ratio of $donor_{BPT}/acceptor_{DBT}/acceptor_{NiR}$ = 350:1:1 (Fig. S21, ESI†). And the antenna effect was calculated to be 20.1 (Fig. S23, ESI†), which indicated that the obtained **WP5⊃BPT-DBT-NiR** nanoparticles could function as an efficient sequential light-harvesting antenna in aqueous environment. It is worth mentioning that the antenna effect of this two-step sequential energy transfer was much higher than that of the recently reported two-step ALHSs in aqueous

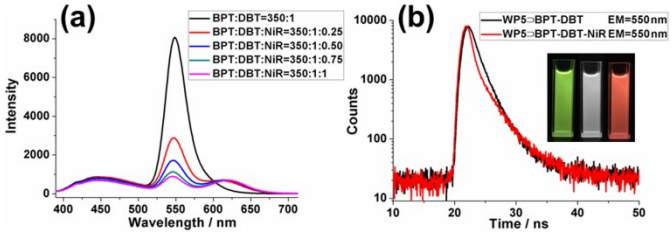

Fig. 6 (a) Fluorescence spectra of **WP5⊃BPT-DBT** nanoparticles in water with different concentrations of **NiR**. (b) Fluorescence decay profiles of **WP5⊃BPT-DBT** nanoparticles (black line) and **WP5⊃BPT-DBT-NiR** nanoparticles (red line). Inset: photographs of **WP5⊃BPT-DBT** nanoparticles, white light fluorescence, and **WP5⊃BPT-DBT-NiR** nanoparticles. [**WP5**] = 2 × 10^{-5} M, [**BPT**] = 1 × 10^{-4} M, [**DBT**] = 2.8 × 10^{-7} M, and [**NiR**] = 2.8 × 10^{-7} M, respectively.

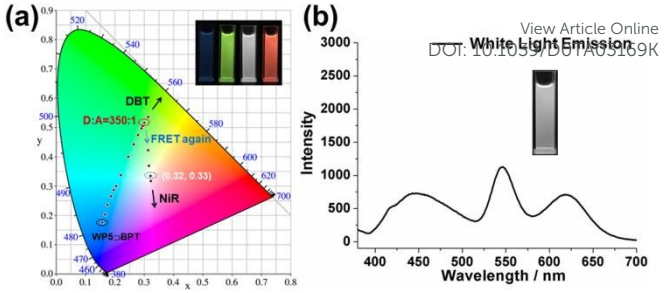

Fig. 7 (a) CIE chromaticity coordinates of **WP5⊃BPT** nanoparticles, **WP5⊃BPT-DBT** nanoparticles with different concentrations of **DBT**, and **WP5⊃BPT-DBT-NiR** nanoparticles with different concentrations of **NiR**. Inset: photographs of **WP5⊃BPT** nanoparticles, **WP5⊃BPT-DBT** nanoparticles, white light fluorescence, and **WP5⊃BPT-DBT-NiR** nanoparticles. (b) Fluorescence spectrum of the white light emission coordinate. [**WP5**] = 2 × 10^{-5} M, [**BPT**] = 1 × 10^{-4} M, [**DBT**] = 2.8 × 10^{-7} M, and [**NiR**] = 2.1 × 10^{-7} M, respectively.

environments.[38,58,59]

Fluorescence lifetime experiments were also performed to investigate the sequential energy transfer process for the **WP5⊃BPT-DBT-NiR** system. The decay curve of the **WP5⊃BPT-DBT** nanoparticles showed the fluorescence lifetimes of τ_1 = 1.36 ns and τ_2 = 2.82 ns when emitting at 550 nm (Fig. 6b and Table S2, ESI†). However, the fluorescence lifetimes of the **WP5⊃BPT-DBT-NiR** nanoparticles further decreased to τ_1 = 1.11 ns and τ_2 = 2.38 ns (Table S2, ESI†) when emitting at 550 nm, indicating that a potential two-step sequential artificial light-harvesting system was successfully created and the energy could be efficiently transferred from the **WP5⊃BPT-DBT** assembly to the second acceptor **NiR**.

Investigation of the fluorescence emission color of supramolecular nanoparticles

Subsequently, the fluorescence emission behavior of the **WP5⊃BPT-DBT-NiR** nanoparticles was investigated. Since the emission color of the **WP5⊃BPT-DBT-NiR** nanoparticles is mainly relied on the fluorescence spectrum output, it is hard to judge the perceived color changes of the overall emission from the spectral evolution.[50] Fortunately, based on the CIE (Commission Internationale de l'Eclairage) 1931 chromaticity diagram, it will be easy to depict the emission color changes by converting each spectrum to a CIE coordinate and mapping the coordinates on the corresponding CIE diagram.[48,50,73] As shown in Fig. 7, the **WP5⊃BPT** nanoparticles lay in light blue area without the presence of acceptor. However, with the ratio of **DBT** increased from 6500:1 to 350:1, the emission color of the **WP5⊃BPT-DBT** system changed from light blue to bright green gradually (Fig. 7a and S26, ESI†), indicating an efficient energy transfer process occurred from the **WP5⊃BPT** assembly to **DBT**. Furthermore, similar to the one-step energy transfer process, the sequential energy transfer from the **WP5⊃BPT-DBT** nanoparticles ($Donor_{BPT}$/$Acceptor_{DBT}$ = 350:1) to **NiR** could be observed directly, and during this process the emission color changed from bright green to bright red (Fig. 7a and S26, ESI†). The above results expressed the emission color coordinates were related to the FRET process, which was induced by the remarkable AIE effect of the **WP5⊃BPT** assembly. Notably, during this two-step sequential energy transfer process, a strong white light emission could be obtained at a concentration of 0.1 mM (**BPT**) with the moral ratio of [**BPT**]/[**DBT**]/[**NiR**] = 350:1:0.75 (Fig. 6 and 7). The emission color coordinate of the **WP5⊃BPT-DBT-NiR** nanoparticles was calculated to be (0.32, 0.33) (Fig. 7a), which is very close to the exact white point (0.33, 0.33), showing a potential application in white-light emission materials. Furthermore, under this condition, the second-step sequential energy transfer efficiency from the **WP5⊃BPT-DBT** nanoparticles to **NiR** was 86.5% and the fluorescence quantum yield of the **WP5⊃BPT-DBT-NiR** nanoparticles was 23.49% (Fig. S24 and S25, ESI†), indicating the successful construction of a white-light emission material based on a two-step sequential energy transfer process. Moreover, such a supramolecular system possessed a strong ability of white fluorescence emission and promising applications in visible-light photocatalysis.[38,54,74-77]

Conclusions

In summary, we have successfully constructed a two-step sequential aqueous light-harvesting system with excellent efficiency based on supramolecular self-assembly, which showed an ultrahigh antenna effect of 47.8 (first step) and 20.1 (second step) with a high donor/acceptor ratio ([**BPT**]/[**DBT**] = 350:1 and [**BPT**]/[**DBT**]/[**NiR**] = 350:1:1). Firstly, a novel one-step artificial light-harvesting system (**WP5⊃BPT-DBT** assembly) was fabricated, which showed enhanced AIE effect and could function as an ideal donor to realize the first-step of the energy transfer from **WP5⊃BPT** assembly to **DBT**. Moreover, inspired by the sequential energy transfer in nature, **NiR** was carefully selected as the second acceptor to fabricate an efficient two-step sequential light-harvesting system based on **WP5⊃BPT-DBT-NiR** assembly, which exhibited a high FRET

efficiency of 60.9% and 89.4% for the two-step sequential energy transfer process, respectively. Notably, the fluorescence emission changed from light blue to bright green and then to bright red during this process, thus by tuning the molar ratio of **DBT** and **NiR**, a bright white light emission can be achieved, which showed a strong ability of white fluorescence emission and promising application in visible-photocatalysis. This work provides a novel approach for the construction of a highly efficient two-step sequential light-harvesting system in aqueous phase based on supramolecular self-assembly, which possesses an excellent FRET efficiency and has great potential application in the fields of mimicking multi-step energy transfer process in nature.

Experimental

Fabrication of different supramolecular nanoparticle solutions

Initially, the stock solution of **BPT** (0.02 M, dissolved in DMSO), **WP5** (4.2×10^{-4} M, dissolved in water), **DBT** (2×10^{-4} M, dissolved in DMSO), and **NiR** (2×10^{-4} M, dissolved in DMSO) were prepared, respectively. **WP5⊃BPT** nanoparticles were prepared as follows: 25 μL of **BPT** and 240 μL of **WP5** solution were added into 4.76 mL of water to generate the assembly solutions during ultrasonication within 30 s. **WP5⊃BPT-DBT** nanoparticles were prepared as follows: 25 μL of **BPT**, 7 μL of **DBT**, and 240 μL of **WP5** solution was added into 4.76 mL of water to generate the assembly solutions during ultrasonication within 30 s. **WP5⊃BPT-DBT-NiR** nanoparticles were prepared as follows: 25 μL of **BPT**, 7 μL of **DBT**, 7 μL of **NiR**, and 240 μL of **WP5** solution was added into 4.76 mL of water to generate the assembly solutions during ultrasonication within 30 s.

Fabrication of white light emission

Initially, the stock solution of **BPT** (0.02 M, dissolved in DMSO), **WP5** (4.2×10^{-4} M, dissolved in water), **DBT** (2×10^{-4} M, dissolved in DMSO), and **NiR** (2×10^{-4} M, dissolved in DMSO) were prepared, respectively. White light emission solutions were prepared as follows: 25 μL of **BPT**, 7 μL of **DBT**, 5.3 μL of **NiR**, and 240 μL of **WP5** solution were added into 4.76 mL of water to generate the assembly solutions during ultrasonication within 30 s.

Conflicts of interest

There are no conflicts to declare.

Acknowledgements

This work was supported by the National Natural Science Foundation of China (No. 21871136), and the Natural Science Foundation of Jiangsu Province (No. BK20180055). Guangping Sun is grateful to Mr. Zhengpeng Hu for the helpful discussion about synthesis.

References

View Article Online
DOI: 10.1039/D0TA03169K

1 H. Nilsson, F. Rappaport and A. Boussac, *Nat. Commun.*, 2014, **5**, 4305–4311.
2 A. Mahapatra, D. Prochowicz, M. M. Tavakoli, S. Trivedi, P. Kumar and P. Yadav, *J. Mater. Chem. A*, 2020, **8**, 27–54.
3 G. D. Scholes, G. R. Fleming, A. Olaya-Castro and R. V. Grondelle, *Nat. Chem.*, 2011, **3**, 763–774.
4 T. Kondo, A. Pinnola, W. Chen, L. Dall'Osto, R. Bassi and G. S. Schlau-Cohen, *Nat. Chem.*, 2017, **9**, 772–778.
5 M. Schulze, V. Kunz, P. D. Frischmann and F. Würthner, *Nat. Chem.*, 2016, **8**, 576–583.
6 N. E. Holt, D. Zigmantas, L. Valkunas, X.-P. Li, K. K. Niyogi and G. R. Fleming, *Science*, 2005, **307**, 433–436.
7 Q. Zou, K. Liu, M. Abbas and X. Yan, *Adv. Mater.*, 2016, **28**, 1031–1043.
8 Y.-H. Jeong, M. Son, H. Yoon, P. Kim, D.-H. Lee, D. Kim and W.-D. Jang, *Angew. Chem. Int. Ed.*, 2014, **53**, 6925–6928.
9 W.-Q. Wu, H.-L. Feng, H.-S. Rao, Y.-F. Xu, D.-B. Kuang and C.-Y. Su, *Nat. Commun.*, 2014, **5**, 3968–3976.
10 K. V. Rao, K. K. R. Datta, M. Eswaramoorthy and S. J. George, *Angew. Chem. Int. Ed.*, 2011, **50**, 1179–1184.
11 R. Sethy, J. Kumar, R. Métivier, M. Louis, K. Nakatani, N. M. T. Mecheri, A. Subhakumari, K. G. Thomas, T. Kawai and T. Nakashima, *Angew. Chem. Int. Ed.*, 2017, **56**, 15053–15057.
12 C. Felip-León, S. Díaz-Oltra, F. Galindo and J. F. Miravet, *Chem. Mater.*, 2016, **28**, 7964–7972.
13 N. Aratani, D. Kim and A. Osuka, *Acc. Chem. Res.*, 2009, **42**, 1922–1934.
14 Y. Nakamura, N. Aratani and A. Osuka, *Chem. Soc. Rev.*, 2007, **36**, 831–845.
15 J. Yang, M.-C. Yoon, H. Yoo, P. Kim and D. Kim, *Chem. Soc. Rev.*, 2012, **41**, 4808–4826.
16 S. H. Lee, A. J. Matula, G. Hu, J. L. Troiano, C. J. Karpovich, R. H. Crabtree, V. S. Batista and G. W. Brudvig, *ACS Appl. Mater. Interfaces*, 2019, **11**, 8000–8008.
17 P. K. Dutta, S. Levenberg, A. Loskutov, D. Jun, R. Saer, J. T. Beatty, S. Lin, Y. Liu, N. W. Woodbury and H. Yan, *J. Am. Chem. Soc.*, 2014, **136**, 16618–16625.
18 F. Garo and R. Häner, *Angew. Chem. Int. Ed.*, 2012, **51**, 916–919.
19 L. Zhao, H. Zou, H. Zhang, H. Sun, T. Wang, T. Pan, X. Li, Y. Bai, S. Qiao, Q. Luo, J. Xu, C. Hou and J. Liu, *ACS Nano*, 2017, **11**, 938–945.
20 H.-Q. Peng, L.-Y. Niu, Y.-Z. Chen, L.-Z. Wu, C.-H. Tung and Q.-Z. Yang, *Chem. Rev.*, 2015, **115**, 7502–7542.
21 M. E. Foster, J. D. Azoulay, B. M. Wong and M. D. Allendorf, *Chem. Sci.*, 2014, **5**, 2081–2090.
22 V. M. Suresh, S. J. George and T. K. Maji, *Adv. Funct. Mater.*, 2013, **23**, 5585–5590.
23 X. Zhang, M. A. Ballem, Z.-J. Hu, P. Bergman and K. Uvdal, *Angew. Chem. Int. Ed.*, 2011, **50**, 5729–5733.
24 S. Bhattacharyya, B. Jana and A. Patra, *ChemPhysChem*, 2015, **16**, 796–804.
25 D. Zhang, Y. Liu, Y. Fan, C. Yu, Y. Zheng, H. Jin, L. Fu, Y. Zhou and D. Yan, *Adv. Funct. Mater.*, 2016, **26**, 7652–7661.

26 M. K. Barman, B. Paramanik, D. Bain and A. Patra, *Chem. Eur. J.*, 2016, **22**, 11699–11705.
27 G. Chadha, Q.-Z. Yang and Y. Zhao, *Chem. Commun.*, 2015, **51**, 12939–12942.
28 P.-Z. Chen, Y.-X. Weng, L.-Y. Niu, Y.-Z. Chen, L.-Z. Wu, C.-H. Tung and Q.-Z. Yang, *Angew. Chem. Int. Ed.*, 2016, **55**, 2759–2763.
29 R. Croce and H. V. Amerongen, *Nat. Chem. Biol.*, 2014, **10**, 492–501.
30 Y. Liu, J. Jin, H. Deng, K. Li, Y. Zheng, C. Yu and Y. Zhou, *Angew. Chem. Int. Ed.*, 2016, **55**, 7952–7957.
31 J. Luo, Z. Xie, J. W. Y. Lam, L. Cheng, H. Chen, C. Qiu, H. S. Kwok, X. Zhan, Y. Liu, D. Zhu and B. Tang, *Chem. Commun.*, 2001, **18**, 1740–1741.
32 J. Mei, N. L. C. Leung, R. T. K. Kwok, J. W. Y. Lam and B. Tang, *Chem. Rev.*, 2015, **115**, 11718–11940.
33 B. Li, T. He, X. Shen, D. Tang and S. Yin, *Polym. Chem.*, 2019, **10**, 796–818.
34 C. W. Kang, D. H. Lee, Y. J. Shin, J. Choi, Y.-J. Ko, S. M. Lee, H. J. Kim, K. C. Ko and S. U. Son, *J. Mater. Chem. A*, 2018, **6**, 17312–17317.
35 K. S. N. Kamaldeep, S. Kaur, V. Bhalla, M. Kumar and A. Gupta, *J. Mater. Chem. A*, 2014, **2**, 8369–8375.
36 G. Liang, F. Ren, H. Gao, F. Zhu, Q. Wu and B. Tang, *J. Mater. Chem. A*, 2017, **5**, 2115–2122.
37 X. Zhu, J.-X. Wang, L.-Y. Niu and Q.-Z. Yang, *Chem. Mater.*, 2019, **31**, 3573–3581.
38 M. Hao, G. Sun, M. Zuo, Z. Xu, Y. Chen, X.-Y. Hu and L. Wang, *Angew. Chem. Int. Ed.*, 2019, **58**, 2–8.
39 M. Zhu, Y. Zhuo, K. Cai, H. Guo and F. Yang, *Dyes Pigments*, 2017, **14**, 343–349.
40 L. Lin, X. Lin, H. Guo and F. Yang, *Org. Biomol. Chem.*, 2017, **15**, 6006–6013.
41 J. Otsuki, *J. Mater. Chem. A*, 2018, **6**, 6710–6753.
42 K. E. Sapsford, L. Berti and I. L. Medintz, *Angew. Chem. Int. Ed.*, 2006, **45**, 4562–4588.
43 J. Wang, S. Liu, Z. Chai, K. Chang, M. Fang, M. Han, Y. Wang, S. Li, H. Han, Q. Li and Z. Li, *J. Mater. Chem. A*, 2018, **6**, 22256–22265.
44 I. Tosi, B. Bardi, M. Ambrosetti, E. Domenichini, A. Iagatti, L. Baldini, C. Cappelli, M. D. Donato, F. Sansone, C. Sissa and F. Terenziani, *Dyes Pigments*, 2019, **171**, 107652–107662.
45 Z. Xun, T. Yu, Y. Zeng, J. Chen, X. Zhang, G. Yang and Y. Li, *J. Mater. Chem. A*, 2015, **3**, 12965–12971.
46 Y. Liu, L. You, F. Lin, K. Fu, W. Yuan, E.-Q. Chen, Z.-Q. Yu and B. Tang, *ACS Appl. Mater. Interfaces*, 2019, **11**, 3516–3523.
47 L.-B. Meng, D. Li, S. Xiong, X.-Y. Hu, L. Wang and G. Li, *Chem. Commun.*, 2015, **51**, 4643–4646.
48 Z. Xu, S. Peng, Y.-Y. Wang, J.-K. Zhang, A. I. Lazar and D.-S. Guo, *Adv. Mater.*, 2016, **28**, 7666–7671.
49 H.-Q. Peng, J.-F. Xu, Y.-Z. Chen, L.-Z. Wu, C.-H. Tung and Q.-Z. Yang, *Chem. Commun.*, 2014, **50**, 1334–1337.
50 W.-C. Geng, Y.-C. Liu, Y.-Y. Wang, Z. Xu, Z. Zheng, C.-B. Yang and D.-S. Guo, *Chem. Commun.*, 2017, **53**, 392–395.
51 J.-J. Li, Y. Chen, J. Yu, N. Cheng and Y. Liu, *Adv. Chem.*, 2017, **29**, 1701905–1701909.
52 S. Guo, Y. Song, Y. He, X.-Y. Hu and L. Wang, *Angew. Chem. Int. Ed.*, 2018, **57**, 3163–3167.
53 Y. Li, Y. Dong, L. Cheng, C. Qin, H. Nian, H. Zhang, Y. Yu and L. Cao, *J. Am. Chem. Soc.*, 2019, **141**, 8412–8415.
54 Z. Zhang, Z. Zhao, Y. Hou, H. Wang, X. Li, G. He and M. Zhang, *Angew. Chem. Int. Ed.*, 2019, **131**, 8954–8958.
55 H.-Q. Peng, Y.-Z. Chen, Y. Zhao, Q.-Z. Yang, L.-Z. Wu, C.-H. Tung, L.-P. Zhang and Q.-X. Tong, *Angew. Chem. Int. Ed.*, 2012, **51**, 2088–2092.
56 L. Ji, Y. Sang, G. Ouyang, D. Yang, P. Duan, Y. Jiang and M. Liu, *Angew. Chem. Int. Ed.*, 2019, **58**, 844–848.
57 X. Wei, X. Su, P. Cao, X. Liu, W. Chang, M. Li, X. Zhang and Z. Liu, *Nature*, 2016, **534**, 69–74.
58 Z. Xu, D. Gonzalez-Abradelo, J. Li, C. A. Strassert, B. J. Ravoo and D.-S. Guo, *Mater. Chem. Front.*, 2017, **1**, 1847–1852.
59 S. Afzal, M. S. Lone, P. A. Bhat and A. A. Dar, *J. Photochem. Photobiol. A Chem.*, 2018, **365**, 220–231.
60 M. K. Dhinakaran, W. Gong, Y. Yin, A. Wajahat, X. Kuang, L. Wang and G. Ning, *Polym. Chem.*, 2017, **8**, 5295–5302.
61 S. K. Bhaumik and S. Banerjee, *Chem. Commun.*, 2020, **56**, 655–658.
62 R. Hu, N. L. C. Leung and B. Tang, *Chem. Soc. Rev.*, 2014, **43**, 4494–4562.
63 G. Sun, Z. He, M. Hao, Z. Xu, X.-Y. Hu, J.-J. Zhu and L. Wang, *Chem. Commun.*, 2019, **55**, 10892–10895.
64 G. Sun, Z. He, M. Hao, M. Zuo, Z. Xu, X.-Y. Hu, J.-J. Zhu and L. Wang, *J. Mater. Chem. B*, 2019, **7**, 3944–3949.
65 C. Ding, Y. Liu, T. Wang and J. Fu, *J. Mater. Chem. B*, 2016, **4**, 2819–2827.
66 M. Zuo, W. Qian, T. Li, X.-Y. Hu, J. Jiang, and L. Wang, *ACS Appl. Mater. Interfaces*, 2018, **10**, 39214–39221.
67 D. V. Berdnikova, N. I. Sosnin, O. A. Fedorova and H. Ihmels, *Org. Biomol. Chem.*, 2018, **16**, 545–554.
68 X. Liu, K. Jia, Y. Wang, W. Shao, C. Yao, L. Peng, D. Zhang, X.-Y. Hu and L. Wang, *ACS Appl. Mater. Interfaces*, 2017, **9**, 4843–4850.
69 W. Shao, X. Liu, G. Sun, X.-Y. Hu, J.-J. Zhu and L. Wang, *Chem. Commun.*, 2018, **54**, 9462–9465.
70 X.-Y. Hu, M. Ehlers, T. Wang, E. Zellermann, S. Mosel, H. Jiang, J.-E. Ostwaldt, S. K. Knauer, L. Wang and C. Schmuck, *Chem. Eur. J.*, 2018, **24**, 9754–9759.
71 L. Gao, T. Wang, K. Jia, X. Wu, C. Yao, W. Shao, D. Zhang, X.-Y. Hu and L. Wang, *Chem. Eur. J.*, 2017, **23**, 6605–6614.
72 T. Xiao, W. Zhong, L. Zhou, L. Xu, X.-Q. Sun, R. B. Elmes, X.-Y. Hu and L. Wang, *Chin. Chem. Lett.*, 2019, **30**, 31–36.
73 L. Xu, Z. Wang, R. Wang, L. Wang, X. He, H. Jiang, H. Tang, D. Cao and B. Tang, *Angew. Chem. Int. Ed.*, 2019, **58**, 1–6.
74 V. Srivastava, P. K. Singh, S. Kanaujia and P. P. Singh, *New J. Chem.*, 2018, **42**, 688–691.
75 V. Srivastava, P. K. Singh and P. P. Singh, *Tetrahedron Lett.*, 2019, **60**, 40–43.
76 M. Neumann, S. Füldner, B. König and K. Zeitler, *Angew. Chem. Int. Ed.*, 2011, **50**, 951–954.
77 Z. J. Wang, S. Ghasimi, K. Landfester and K. A. I. Zhang, *J. Mater. Chem. A*, 2014, **2**, 18720–18724.

View Article Online
DOI: 10.1039/D0TA03169K

Graphical Abstract

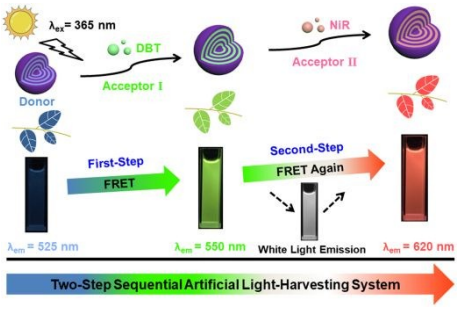

An efficient artificial light-harvesting system with two-step sequential energy transfer has been successfully constructed based on supramolecular self-assembly.